Title

Determining the long-term operational performance of pump and treat and the possibility of closure for a large TCE plume.

Authors
Guo, Zhilin
Brusseau, Mark L
Fogg, Graham E

Publication Date
2019-03-01

DOI
10.1016/j.jhazmat.2018.11.057

Peer reviewed

Journal of Hazardous Materials 365 (2019) 796–803

Contents lists available at ScienceDirect

Journal of Hazardous Materials

journal homepage: www.elsevier.com/locate/jhazmat

Determining the long-term operational performance of pump and treat and the possibility of closure for a large TCE plume

Zhilin Guo[a,*], Mark L. Brusseau[b], Graham E. Fogg[a]

[a] Land, Air, and Water Resources, University of California, Davis, 1 Shields Ave, Davis, CA, 95616, United States
[b] Soil, Water and Environmental Science Department, University of Arizona, 429 Shantz Bldg., Tucson, AZ, 85721, United States

ARTICLE INFO

Keywords:
Long-term management
Pump and treat
Rebound

ABSTRACT

The purpose of this study is to evaluate the impact of heterogeneity on the long-term performance of a large pump-and-treat (PAT) system that has been in operation for 30 years at a site located in Tucson, AZ. A 3D numerical model was developed. Three different concentrations were examined: composite concentration in the influent to the treatment plant, resident concentration in the aquifer, and concentration for downgradient boundary discharge. The time scales needed for concentrations measured in these ways to reach the Maximum Contaminant Levels (MCLs) are significantly different, with ~125 years required for treatment-plant influent compared to ~225 years for downgradient boundary discharge and > > 227 years (total simulated time) for the resident concentration in the aquifer. These large time scales, compared to 36 years for a hypothetical homogeneous system, demonstrate the significant impacts of permeability heterogeneity on remediation at this site. The possibility of closure of the site was investigated by examining the mass discharge from the site boundary and the concentration rebound after simulating shutdown of the PAT system. The results of this study provide insight on evaluation of closure potential for large, complex contamination sites and a reference on selecting performance metrics for site management.

1. Introduction

Groundwater resources contaminated by a variety of organic and inorganic contaminants used in industrial, commercial, agriculture, and other applications continue to pose significant threats to human health and the environment. Examples of compounds of concern include chlorinated solvents (e.g., trichloroethene, tetrachloroethene, carbon tetrachloride), 1,4-dioxane, methyl tertiary-butyl ether (MTBE), and perchlorate. The transport processes of these contaminants are highly impacted by the heterogeneity and anisotropy of alluvial subsurface environments [e.g., 1–13]. Extensive dissolved-phase plumes typically form at sites contaminated by these constituents, which has been reported in many previous studies [e.g., 6,7,14–17]. These large plumes are very expensive to contain or completely cleanup, posing long-term constraints to site management and closure.

It is now recognized that most sites with large groundwater plumes comprising these contaminants will require many decades before cleanup will be achieved under current methods and standards [e.g., 18]. This realization has resulted in the search for more cost-effective alternatives to pump and treat. However, there are only few options that work effectively for large, deep plume besides PAT, including modified permeable reactive barriers (PRBs) emplaced using wells and monitored natural attenuation (MNA) or enhanced attenuation (EA).

PRBs have been successfully applied at contamination sites with organic and inorganic contaminants with proper design of the PRB systems [e.g., 19–23]. However, most of these reported applications are for sites wherein contaminants are residing in relatively shallow aquifers, i.e. less than 20 m deep. PRB systems can fail because of incomplete hydraulic capture due to insufficient depth or width, as demonstrated for projects reported in Henderson and Demond [24] and other factors, such as inappropriate reactive media and inadequate maintenance of the structure [e.g., 20,25,26]. Therefore, PRBs are typically not be suitable for sites with deep, wide plumes and sites needing long-term intensive remediation. MNA has been widely accepted as a potential alternative to pump and treat because of the lower cost for large, complex plumes. However, whether MNA can effectively prevent further migration of the plume after PAT is shut down needs to be evaluated and verified for each applications [18]. Therefore, how to contain or remove contaminants for sites with large, complex plumes efficiently and effectively with these few options available is one of the most critical issues in subsurface remediation. Clearly, groundwater models that adequately represent transport phenomena are needed to

* Corresponding author: Department of Land, Air, and Water Resources, University of California, Davis, CA, 95616, United States.
E-mail address: zlguo@ucdavis.edu (Z. Guo).

https://doi.org/10.1016/j.jhazmat.2018.11.057
Received 10 June 2018; Received in revised form 20 October 2018; Accepted 15 November 2018
Available online 16 November 2018
0304-3894/

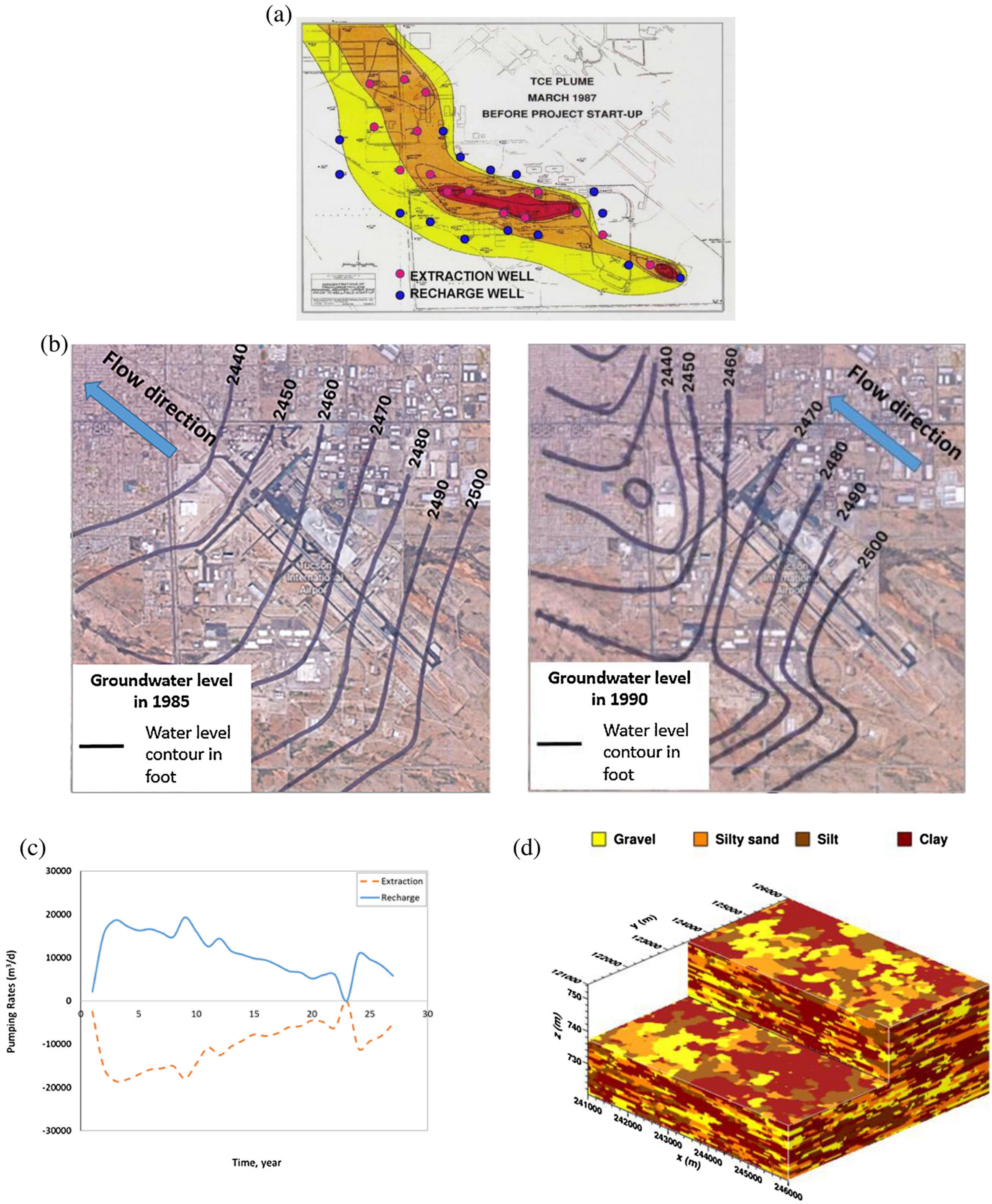

Fig. 1. Study domain and TCE plume map at the site: (a) TCE plume as 1987; (b) Groundwater levels (foot) before PAT initiated (1985) and after (1990). (c) Extraction and recharge rates (m^3/d) for past 27 years. (d) Simulated heterogeneous domain.

support the long-term evaluation of groundwater quality and to identify decadal time-scale management strategies.

In alluvium sites, flow fields are strongly impacted by material heterogeneity, which will further affect transport processes such as the mass transfer between the well-connected highly permeable materials and the low-permeability materials. The early arrival of contaminants caused by preferential flow in well-connect channels and the asymptotical tails resulting from transport through and mass-transfer to and from low-permeability materials have been frequently observed, which significantly challenges long-term management [e.g., 5,6,8–13,27,28]. Therefore, a groundwater model that represents highly heterogeneous geologic and hydrogeologic systems is needed for reliable characterization and prediction of groundwater flow and to obtain accurate representation of remediation responses. However, detailed information to describe heterogeneity and anisotropy for a regional scale field is difficult and costly to obtain due to spatial variability of the subsurface and the relative scarcity of data on media properties.

Geostatistical and stochastic methods have been developed using geostatistical parameters deduced from available data, which are collected from borehole logs, pumping tests, and other means, to delineate the spatial distribution of hydraulic conductivity that can be incorporated into flow and transport. Fogg and colleagues [29–32] developed the transition probability Markov chain approach, which incorporates indicator geostatistical methods with the available site information relating to textural and depositional facies, to characterize and simulate the heterogeneity. The method has been demonstrated to provide reasonable representation for highly heterogeneous sites in previous studies.

In addition to characterization of the aquifer heterogeneity, it is also critical to accurately simulate contaminant migration including the mass transfer into and out of the fine materials for which transport is dominated by diffusion. Labolle and Fogg [28] demonstrated the important role of diffusion in low permeability zones and the impact on PAT at alluvial sites. However, very few models [e.g., 2,13,28] include diffusion for PAT simulations because of the difficulty of handling the diffusive mass transfer processes in heterogeneous media at large scales.

Guo et al. [33] used a geostatistical method to represent permeability heterogeneity of a TCE-contamination site, and evaluated the effectiveness of different transport modeling methods to simulate 27 years of PAT system operation. This work will extend the study to investigate the long-term performance of the current PAT system. This study uniquely presents analysis of long-term, high-resolution historical pump-and-treat data using high-resolution representation of permeability heterogeneity to evaluate the performance of PAT, estimate the time scale for site closure, and explore the possibility for alternative strategies such as MNA. This work discusses the appropriate performance metric for site management for the first time by comparing three different concentrations: composite concentration in the influent to the treatment plant, resident concentration in the aquifer, and concentration in groundwater flowing out of the downgradient site boundary.

2. Method

2.1. Site description

The selected site is part of the Tucson International Airport Area (TIAA) federal Superfund site in southern Arizona. TCE entered the subsurface by seepage from unlined pits and other features used for the disposal of organic solvents during the 1940′s to mid-1970′s. In the early 1980′s, TCE was detected in groundwater from several potable water supply wells. A large, multiple-source plume of TCE exists in the upper portion of the regional aquifer. The TIAA site was placed on the National Priorities List in 1983 and divided into three major zones, the North, Central, and South sections administratively [34]. The current study site is located within the south section of the site. PAT systems are in independent operation in both the north and south sections.

The groundwater plume at the study site was approximately 5.5 km long and 1.0 km wide (Fig. 1a) within the regional aquifer before the initiation of remediation activities in 1987 [35]. This aquifer comprises alluvial sediments and is located along the western edge of the Tucson Basin [36,37]. Four hydrogeologic units are defined at the site, the unsaturated zone, 0 to 20 m below ground surface (m bgs); the upper zone (UZ) of the local aquifer, 20 to 60 m bgs; confining unit, 60 to 90 m bgs, and the lower zone (LZ) of the local aquifer, 90 m bgs to an unknown depth [38]. The potentiometric surface of the shallow groundwater zone is 28 ~ 29 m below land surface (bls). The groundwater flows from southeast to northwest induced by natural gradient of 0.007 before PAT was initiated (Fig. 1b). The local flow field has been changed because of the extraction-recharge process of the PAT system (Fig. 1b), but the regional flow remains to northwest direction. The TCE contaminants reside primarily in the UZ, which consists of clay and silty clay units, sand and/or gravel units, and an underlying, laterally extensive, clay unit starting at ~37 m bls separating the shallow groundwater zone from the regional aquifer [37]. Prior site-characterization activities indicate that solvent fluid was present in the source zones at the site [5,39].

Aqueous concentrations of TCE as high as thousands of ug/L have been reported for groundwater sampled from monitoring wells. Various remediation programs have been in operation at different parts of the site over the past 30 years. The PAT system was initiated in 1987 with 24 extraction wells, which are located within source zones and at different regions within the plume, 20 injection wells located primarily along the perimeter of the plume (Fig. 1a), approximately 50 monitoring wells, and groundwater treatment facilities, and remains operational [36]. The total extraction and recharge rates have been declining gradually with time after the first 3 years as shown in Fig. 1d. In the first 10 years, approximately 1 pore volume (PV) of groundwater was extracted, and during the second 10 years, the total extracted water was approximately 0.5 PV. Approximately 2 PV of groundwater has been extracted during the 27 years of PAT operation. The PAT system has been effectively containing and decrease the size of the plume. Approximately 13,000 kg of volatile organic compounds (VOCs) have been removed with the operation of the pump-and-treat system, and the concentration of TCE in groundwater influent to the treatment plant has been reduced to ~25 ug/L from 350 ug/L, which however is still higher than the Maximum Contaminant Level (MCL) of 5 ug/L. A reduction of mass-removal efficiency was observed after the first several years' operation of PAT, showing an asymptotic decrease in TCE concentration in the composite extracted groundwater entering the treatment plant. In-situ chemical oxidation was used for source remediation in 2000 [40]. Soil vapor extraction was conducted in the source zones in the mid 1990′s to early 2000′s.

Based on pumping tests, hydraulic conductivities ranging from 4×10^{-5} to 3×10^{-4} m/s were measured for the gravel sub-unit, and values from 1×10^{-6} to 5×10^{-6} m/s were measured for the primary clay unit above the gravel sub-unit. Natural groundwater flow is from southeast to northwest with natural hydraulic gradients for the gravel sub-unit ranging historically between 5×10^{-3} and 1×10^{-2}.

2.2. Simulation of geologic heterogeneity

The FORTRAN program T-PROGS, which is based on transition probability–Markov chain random-field approach described by Fogg and colleagues [29–32] was used in this study to generate the heterogeneous domain. The hydrofacies categories are identified by interpretation of well logs collected from the site of interest. Transition probabilities are measured and used to conditionally simulate realizations of hydrostratigraphy for each depositional direction (strike, dip and vertical) to generate 3D realizations of random fields. In this study, 245 geological borehole data collected from the TIAA site [41] were interpreted and categorized into four hydrofacies, clay (42.4%), silty sand (17.7%), sand (19.6%), and gravel (20.3%). Vertical lengths were determined directly from the borehole logs whereas strike and dip lengths were estimated through geologic interpretation [31,32]. Mean lengths of the four hydrofacies in the dip, strike and vertical directions are summarized in Table 1.

Based on the resulting Markov chain model of transition probability, the geostatistical conditional realizations were generated on a grid of 250 (strike) x 250 (dip) x 70 (vertical) nodes with 20.0 m x 20.0 m x 0.5 m spacing. The top of the generated domain coincides with the potentiometric surface at the site. Ten realizations were generated

Table 1
Hydraulic conductivity, K, and porosity of the four hydrofacies for the heterogeneous simulations.

Hydrofacies	K, m/d	Porosity	Direction and mean length		
			Strike (m)	Dip (m)	Vertical (m)
Coarse Grain	124	0.2	360	500	9.6
Sand	45	0.2	200	265	8.6
Silt	3	0.2	380	350	13.8
Clay	0.00013	0.3	880	700	16.9

randomly to perform the analysis, and one of them is shown in Fig. 1. Because in each of the realizations the coarse aquifer facies comprised by the 39.9% of the system containing sands or gravels extensively interconnect in 3D, the overall transport behaviors of preferential flow and late-time tailing did not differ dramatically from realization to realization. Hence, consistent with the findings of LaBolle and Fogg [28], we concluded it was not necessary to do a full stochastic analysis with 100′s of realizations.

2.3. Groundwater flow model

Groundwater flow was simulated using MODFLOW, a 3D numerical (finite-difference) groundwater flow model [42,43]:

$$\frac{\partial}{\partial x}\left(K_{xx}\frac{\partial h}{\partial x}\right)+\frac{\partial}{\partial y}\left(K_{yy}\frac{\partial h}{\partial y}\right)+\frac{\partial}{\partial z}\left(K_{zz}\frac{\partial h}{\partial z}\right)+W=S_s\frac{\partial h}{\partial t} \tag{1}$$

where Kxx, Kyy, and Kzz (L/T) are values of hydraulic conductivity along the x, y, and z coordinate axes; h (L) is the potentiometric head; W (T-1) is a volumetric flux per unit volume representing sources (W > 0) and/or sinks (W < 0) of water. SS (L-1) is the specific storage of the porous material and t is time (T). The aquifer domain was discretized with the same grid as the geostatistical model. General head boundaries were used along the northwest and southeast corners of the domain, with a natural gradient (0.007) inducing lateral groundwater flow from southeast to northwest and no-flow boundaries were defined parallel to the direction of flow. The no-flow boundaries were set far from the area of interest to minimize boundary effects. Spatially variable hydraulic conductivities (K) and porosities are assigned to individual cells according to the categories of hydrofacies for the corresponding cells from the geostatistical realization (Table 1). K and porosities for each hydrofacies used in the model were determined according to information generated from geologic borehole-logs, pumping tests, and historic data collected for the Tucson International Airport Area Superfund site [2].

2.4. Solute transport model

The 3D solute transport in transient groundwater flow systems can be described by the partial differential equation [44]:

$$\frac{\partial(\theta c)}{\partial t}=\frac{\partial}{\partial x_i}\left(\theta D_{ij}\frac{\partial c}{\partial x_j}\right)-\frac{\partial}{\partial x_i}(\theta v_i c)+q_s c_s+\sum r_n \tag{2}$$

where θ (dimensionless) is the porosity of the subsurface medium; c (M/L^3) is the dissolved concentration; $x_{i,\,j}$ (L) is the distance along the respective Cartesian coordinate axis; D (L^2/T) is the hydrodynamic dispersion coefficient tensor, v_i (L/T) is the seepage or linear pore water velocity; q_s (T^{-1}) is the volumetric flow rate per unit volume of aquifer representing fluid sources (positive)/ sinks (negative); c_s (M/L3) is the aqueous solute concentration of the source or sink flux, $\sum r_n$ (M/L^3/T) is the chemical reaction term.

The aqueous diffusion coefficient of 7.6×10^{-5} m^2/d and longitudinal, transverse and vertical dispersivity of 5, 0.5, and 0.05 m were used, respectively. First order kinetics was used for sorption of TCE, with a distribution coefficient of 0.04 cm^3/g and mass transfer coefficient of 15 d^{-1}. The parameters used in the model was determined based on the data measured in the lab experiments for TCE or the site tests reported in Zhang and Brusseau, 1999 [2]. The initial plume was determined according to the TCE distribution in 1987 prior to the commencement of PAT operations and assumed uniform distribution in vertical direction, which is reasonable given that the contaminants resided in the aquifer for several decades.

The simulated composite flux-averaged TCE concentrations for all pumping wells were computed by: compared to the observed composite concentrations measured for the influent to the treatment plant. The flux-averaged concentration for all extraction wells in the system is defined as

$$\overline{C}(t)=\frac{\sum C_i(t)q_i(t)}{\sum q_i(t)} \tag{5}$$

where C_i is the vertically averaged TCE concentration for well i; q_i is the pumping rate for well i. The dissolved-phase concentration c in each cell throughout the entire domain was recorded. The mass distribution of the TCE was then determined by multiplying the pore volume of each cell with the concentration. The mass residing in each hydrofacie was calculated by summing up the mass in cells of the same facies type.

The mass balance was calculated by comparing the total dissolved mass M_{tot} (M), the amount of mass removed (M_{rov}), the amount of mass flowing out of the boundaries (M_{bnd}), the amount of remaining mass in the aqueous phase (M_{ra}), and sorbed phase (M_{rs}), which was calculated by:

$$M_{tot}=M_{rov}+M_{bnd}+M_{ra}+M_{rs} \tag{6}$$

$$M_{tot}=\sum_{j}^{N}C_{j,0}V_j \tag{7}$$

$$M_{rov}=\sum_{i}^{N_w}C_iQ_i\Delta t \tag{8}$$

$$M_{ra}=\sum_{j}^{N}C_jV_j \tag{9}$$

$$M_{rs}=(R-1)M_{ra} \tag{10}$$

Where C_j (M^3/L) is the concentration in the j^{th} cell, and N is the total number of cells. $C_{j,0}$ (M^3/L) is the initial concentration in the j^{th} cell. V_j (L^3) is the pore volume in the j^{th} cell. N_w is the total number of wells. Q_i is the pumping rate of i^{th} well. Δt is the time period that concentration data was monitored, monthly data was used in this study. R is the retardation factor, which is described by:

$$R=1+\frac{\rho_b}{\theta}K_d \tag{11}$$

Where K_d (L^3/M) is the distribution coefficient and ρ_b (M/L^3) is the bulk density of the subsurface medium.

2.5. Simulations

Three different scenarios were simulated for pump-and-treat operations at the site— (I) Actual operation period, (II) Extended operation to completion of remedial objective, and (III) Shut down of pump and treat. For scenario I, 27 stress periods were used to simulate 27 years of PAT from 1987 to 2013. Separate simulations were conducted for the heterogeneous field generated using the stochastic method discussed in Section 2.2, and for a homogeneous control domain. Pumping rates for wells, recorded continuously and tabulated monthly throughout the course of operation, from 1987 to 2013 were used as input.

For scenario II, the simulation time was extended to 200 years and the pumping rates for 2013 were used for the remainder of the simulated operation. The purpose of this simulation was to examine the time scale required for the site to achieve the remediation goal, reducing groundwater TCE concentration below MCLs 0.005 mg/L. Three different concentrations were examined: composite concentration in the influent to the treatment plant, resident concentration in the aquifer, and concentration in groundwater flowing out of the downgradient site boundary.

For scenario III, the operation of the PAT system from 1987 to 2013 was first simulated identically to scenario I. Then, the PAT system was turned off and the concentrations were monitored for 50 years. The purpose of this simulation is to test the management option of reducing remediation costs by shutting down the PAT system. The option is

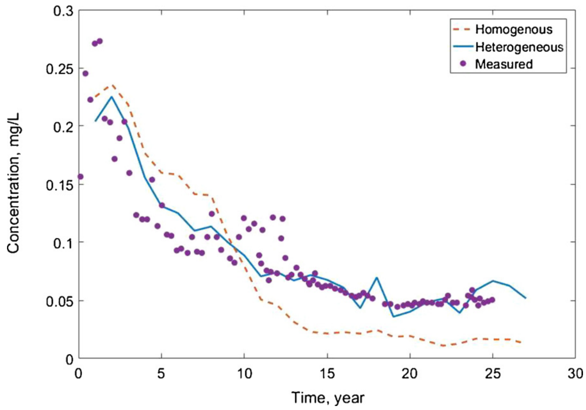

Fig. 2. Composite TCE concentrations of influent to the treatment plant for observed data, homogeneous simulation, and heterogeneous simulation.

based on the ability of natural attenuation to minimize contaminant concentrations leaving the site, in combination with capture of off-site contamination by the PAT system operating in the north section of the TIAA site. The same three sets of concentrations were examined as for scenario II.

3. Results

3.1. Impact of heterogeneity on remediation efficiency

The elution curves for both heterogeneous and homogeneous simulations are presented in Fig. 2. The measured composite TCE concentration in the influent to the treatment plant increased significantly during the first year of operation as the PAT system stabilized. The concentration then began to drop relatively rapidly over the next 5 years. The rate of concentration decline slowed thereafter, exhibiting asymptotic conditions over the next approximately 15 years. Steady-state conditions have been observed over the past 5 years wherein concentrations have remained essentially unchanged. This time period is equivalent to approximately 2 pore volumes (PV) of water extraction. The asymptotic behavior is due to heterogeneity and continued supply from source zones [2,5]. The results from the heterogeneous simulation provide a good match to the measured elution curve.

The concentrations for the homogeneous simulation are higher in early years compared to the concentrations for the heterogeneous simulation and drop to lower values after approximately 10 years of pumping (after ~1 pore volume). The differences between the two elution curves are attributed to the large magnitude of permeability heterogeneity present at the site. Given the significant impact of heterogeneity, it is critical to represent heterogeneity accurately when modeling solute transport, which necessitates the use of a transport model embedding detailed representation of heterogeneity.

For the homogeneous simulation, the decline of concentrations slows down after 20 years of pumping with ~1.5 PV water extracted at ~0.01 mg/L, which is still higher than the MCL of 0.005 mg/L. The asymptotic behavior observed here illustrates the impacts of other factors, such as retardation and well-field hydraulics, on the mass removal behavior. The homogeneous simulation was further extended for 50 years and the concentration drops below the MCLs 0.005 mg/L after 36 years of PAT operation (Fig. 3).

Fig. 3 presents the elution curves for the simulation in which the PAT system operation was extended for 200 years. The concentrations simulated for the influent to the treatment plant (fluxC-well), within the aquifer (C-aquifer), and for groundwater flowing out of the site boundary (fluxC-boundary) are presented. As shown, the time scales for concentrations to reach the MCL are different for the three. It will take approximately 125 years for the flux-averaged concentrations of

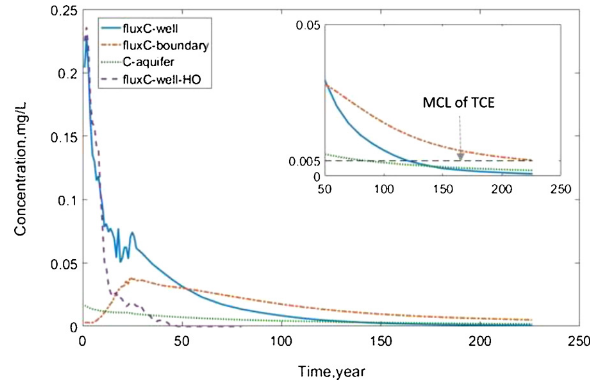

Fig. 3. Elution curves for 200 years of simulation on PAT for the heterogeneous domain showing the time scale needed to achieve the remediation goal. Composite concentrations of influent to the treatment plant (fluxC-well), resident concentrations (C-aquifer), and concentrations for flow discharge from downgradient boundary (fluxC-boundary) are presented. A curve representing hypothetical homogeneous conditions is presented for comparison (fluxC-well − HO).

extraction wells to drop below the MCL, over 225 years for flux-averaged concentrations of water flowing out of the site from the boundary, and even longer for the resident concentration in the aquifer. The large time scales for the heterogeneous simulations compared with the 36 years for the homogenous simulation (fluxC-well − HO) indicate the significant impact of permeability heterogeneity on remediation and the required long-term management at this site.

The large differences between the time scales elicits a question, which concentration should be used as the performance metric for site management? At most sites, the concentrations to the influent of the treatment plant are measured frequently and used to determine the strategies for remediation. However, as shown here, even when the concentrations measured from extraction wells drop below the MCL, there is still contaminated water with higher concentrations escaping the site because of preferential flow paths or insufficient capture achieved by the well field. Moreover, because of the heterogeneity, it is highly likely that high concentrations would persist in low permeability zones after years of operation of PAT. For example, 80% of the contaminant mass remaining in the subsurface resides within low permeability zones (clay and silt) after 27 years of pumping. This will lead to higher resident concentrations in the aquifer.

3.2. Mass balance

The distribution of mass between dissolved mass that was removed via PAT, migrated out of the site at the northern boundary, and remained in the domain as dissolved and sorbed mass during 27 years of groundwater extraction were calculated and plotted in Fig. 4. The measured data that were reported in Brusseau and Guo [11], which examined contaminant-removal behavior at the site using historical contaminant-concentration data collected from the long-term pump-and-treat operations, are also presented. The removed mass in this study is lower than reported values in Brusseau and Guo [11], which is attributed to the presence of DNAPL in the source zone as shown by prior site-characterization activities. In this study, only dissolved and sorbed phase mass was simulated, and as a result, the simulated removed mass was lower than the measured data. Prior and ongoing remedial actions have focused on removing DNAPL mass in the source zones [41]. Based on this, it is assumed that DNAPL in source zones is either not present at quantities to significantly impact PAT removal in the future, or that additional source management will be employed. Hence, the exclusion of NAPL sources is not anticipated to measurably impact the results and discussion in this study.

After 27 years of remediation, approximately two pore volumes of

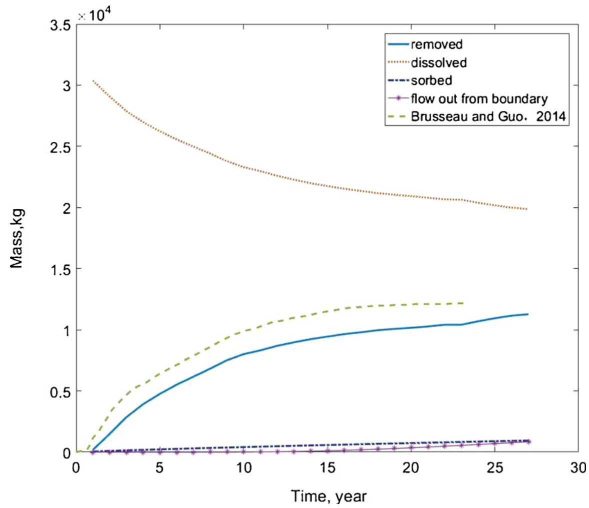

Fig. 4. Mass balance during the operation of PAT.

water was extracted, which is consistent with the data reported in Brusseau and Guo [11]. Over 35% of dissolved mass was removed, leaving 65% in the domain, among which, 66%, 13%, 8%, and 13% of mass resides in the clay, silt, sand, and gravel domains, respectively. This again demonstrates the significant impact from heterogeneity on mass removal and that long-term remediation will be required. During the operation of PAT, approximately 0.2% of mass escapes from the boundary every year. The cumulative mass discharge from the boundary is also presented in Fig. 4.

3.3. Possible shutdown of PAT

The mass discharge from the boundary to the northern part of the TIAA site was calculated and plotted in Fig. 5 for simulations with continuous pumping and ceased pumping after 27 years. This comparison was to test the option of shutting down the PAT system at this site since the current concentration has dropped to a relatively low value and reached steady-state conditions. As the site management at the northern part of the TIAA site continues, the contaminants migrating from the southern region can be captured and treated by the north PAT system. At the same time, MNA will be applied assuming attenuation processes would also effectively reduce the concentration at the site. The key question to address is: would this approach be more cost-effective than continuous operation of the current PAT system at the south complex?

As expected, shutting down the current PAT system results in more contaminant migrating offsite to the northern section compared with the amount of mass migrating to the north for the simulation with continuous pumping (Fig. 5). Moreover, as mentioned in the last section, there is less than 0.2% mass escaping out of the boundary on average every year and the amount has been increasing year by year during the first 20 years of PAT operation. But the increasing rate slowed down, and with continuous pumping, the amount of mass escaping from the boundary starts and continues to decline after 30 years of pumping. For the simulation wherein pumping was turned off after 27 years, mass leaving the site also starts to decrease at year 30, but reaches an asymptotic condition after only 3 years of decline. The persistence of the mass indicates the long-term contamination supply from the southern region since there is no longer containment of the plume.

The amount of mass escaping the boundary after pumping stopped is not as significant as expected, which is due to the water balance between the recharge and extraction for the PAT system. During the operation of PAT system, the amount of groundwater extracted every year is essentially balanced by the amount of water injected. Thus, the groundwater flow field surrounding the remediation site was not impacted significantly. Therefore, after the PAT was shut down, the groundwater flow out from the boundary increased by less than 1 m^3/d from 17.6 m^3/d for the simulation with continuous operation of PAT to 18.5 m^3/d for the simulation wherein pumping ceased after 27 years. But in the long term, because of the continuous mass supply from the uncontained plume, the differences between the continuous and ceased pumping scenarios become larger. This also reflects on the concentration change with time shown in Fig. 6. After the increase of concentrations observed in first 30 years stopped, the concentrations for the simulation with pumping continue to decline, whereas for the ceased-pumping simulation, the concentrations reach an asymptotic condition at approximately 0.03 mg/L.

In addition, rebound is also observed for concentrations monitored at the wells after the pumping stopped at year 28, as shown in Fig. 7. For the simulation wherein pumping stopped, the flux averaged concentration at the locations where the extractions were in first 27 years are used in the figure. The concentrations are more than doubled compared to the concentrations for the simulation with continuous groundwater extraction, which is the result of a) diffusive mass transfer from low permeability zones, b) the migration of the contaminants located in zones wherein the concentration was relatively high without containment. This indicates that without the continuous site management, the groundwater concentration will stay at higher levels for many decades.

4. Summary and conclusion

This study investigated the performance of the PAT system at the TIAA site where a large scale TCE plume exists. A 3D numerical model

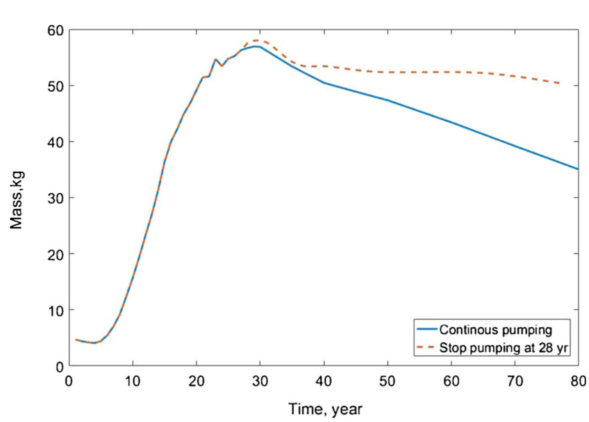

Fig. 5. Mass flow out from the boundary each year for simulations with continuous pumping and ceased pumping at year 28.

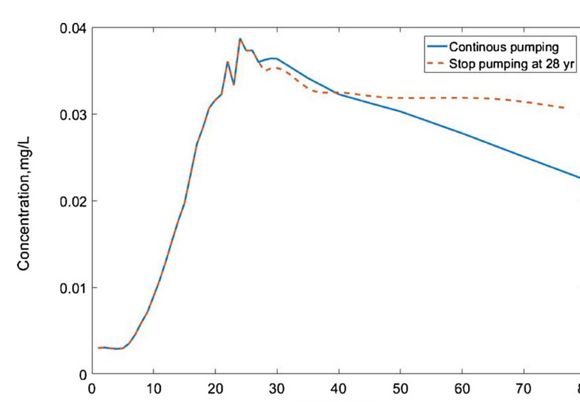

Fig. 6. Concentration across the boundary for simulations with continuous pumping and ceased pumping at year 28.

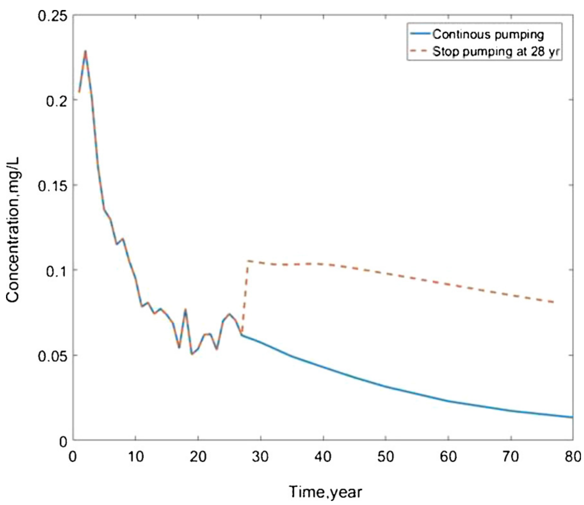

Fig. 7. Concentration rebound for the simulation with ceased pumping at year 28. For year 0–27, the data represent flux composite concentration for extraction wells during PAT; after year 28, the data represent flux composite concentration for natural-gradient conditions.

was developed to simulate the PAT system and the time scale for the site to achieve the remediation goal of concentration reduction to below the MCL. The potential to close the site was investigated by examining the mass discharge from the site boundary and the concentration rebound after PAT system was shut down.

For the first 27 years, the measured pumping rates were incorporated into the model. The relatively close match between the simulated results and the measured concentrations indicates reasonable representation of the site conditions and plume transport behavior in the model. For the forecasting, a constant pumping rate was used, which introduces a source of uncertainty. The forecasting analysis is based on the assumption that the pumping rates and well locations for current PAT system are not changed during the entire simulation period, and also other alternative remediation methods are not considered.

The results demonstrate the significant impacts of heterogeneity on remediation at this site by comparing the elution curves for simulations conducted for the heterogeneous domain and a corresponding homogeneous domain, which also reflects on the time needed ($>$ 125 years) that the concentrations measured in three ways drop below MCLs under current practice. The fact that after 27 years' operation of PAT, almost 80% of contaminants mass remaining in the subsurface resides within low permeability zones also indicates the long-term site manage. The asymptotic behavior observed from the BTC for the homogeneous simulation illustrates the impact from other factors besides permeability heterogeneity. Moreover, for the simulation with continuous pumping, the mass escaping the site declines whereas for the simulation with PAT shutdown, the mass will persist for a long time due to the long-term contamination supply from uncontained high-concentration zones and diffusive mass transfer from extensive low-permeability units present at the site. The concentrations monitored for the aquifer also double after shutting down the PAT. Therefore, the long-term management at the site will be expected under the current remediation practice.

Of note, the time scales needed for concentrations measured in different ways, the influent to the treatment plant, aquifer, and water escaping the site, to reach MCLs are significantly different. In reality, the actual time scales may be different from the ones presented herein because of changes in PAT operations, change of remediation methods, or other potential factors. However, the results from this work provide insights on conducting performance evaluations for site management, especially when examining the possibility of site closure and exploring alternatives. MNA would work effectively to contain the plume only after PAT is operated for a sufficient time and the concentrations in all aspects are sufficiently low. Therefore, complicated evaluations on other alternatives should be done to prevent further migration of the plume before shutting down the PAT at the site.

Acknowledgements

This research was supported by the National Institute of Environmental Health Sciences Superfund Research Program [ES04940], and Department of Energy CERC-WET Program. We thank the reviewers for their constructive comments.

References

[1] G.E. Fogg, E.M. LaBolle, G.S. Weissmann, D.L. Corwin, K. Loague, T.R. Ellsworth (Eds.), Groundwater Vulnerability Assessment: Hydrogeologic Perspective and eXample from Salinas Valley, California, in Assessment of Non-Point Source Pollution in the Vadose Zone,Geophys. Monogr. Ser. vol. 108, AGU, Washington, D. C, 1998, pp. 45–61.
[2] Z.H. Zhang, M.L. Brusseau, Nonideal transport of reactive solutes in Heterogeneous porous media 5. Simulating regional-scale behavior of a trichloroethene plume during pump-and-treat remediation, Water Resour. Res. 35 (1999) 2921–2935.
[3] C.X. Liu, W.P. Ball, Back diffusion of chlorinated solvent contaminants from a natural aquitard to a remediated aquifer under well-controlled field conditions: predictions and measurements, Ground Water 40 (2002) 220-220.
[4] S.W. Chapman, B.L. Parker, Plume persistence due to aquitard back diffusion following dense nonaqueous phase liquid source removal or isolation, Water Resour. Res. 41 (2005) W12411.
[5] M.L. Brusseau, N.T. Nelson, Z. Zhang, J.E. Blue, J. Rohrer, T. Allen, Source-zone characterization of a chlorinated-solvent contaminated superfund site in Tucson, AZ. J. Contam. Hydrol. 90 (2007) 21–40.
[6] M.L. Brusseau, J. Hatton, W. DiGuiseppi, Assessing the impact of source-zone remediation efforts at the contaminant-plume scale through analysis of contaminant mass discharge, J. Contam. Hydrol. 126 (2011) 130–139.
[7] B.L. Parker, S.W. Chapman, M.A. Guilbeault. Plume persistence caused by back diffusion from thin clay layers in a sand aquifer following TCE source-zone hydraulic isolation, J. Contam. Hydrol. 102 (2008) 86–104.
[8] M. Bianchi, C. Zheng, C. Wilson, G.R. Tick, G. Liu, S.M. Gorelick, Spatial connectivity in a highly heterogeneous aquifer: from cores to preferential flow paths, Water Resour. Res. 47 (2011) W05524, , https://doi.org/10.1029/2009WR008966.
[9] M.A. Seyedabbasi, J.C. Newell, D.T. Adamson, T.C. Sale, Relative contribution of DNAPL dissolution and matrix diffusion to the long-term persistence of chlorinated solvent source zones, J. Contam. Hydrol. 134 (2012) 69–81.
[10] R.A. Dearden, D.J. Noy, M.R. Lelliott, R. Wilson, G.P. Wealthall, Release of contaminants from a heterogeneously fractured low permeability unit underlying a DNAPL source zone, J. Contam. Hydrol. 153 (2013) 141–155.
[11] M.L. Brusseau, Z. Guo, Assessing contaminant-removal conditions and plume persistence through analysis of data from long-term pump-and-treat operations, J. Contam. Hydrol. 164 (2014) 16–24.
[12] D.E. Matthieu III, M.L. Brusseau, Z. Guo, M. Plaschke, K.C. Carroll, F. Brinker, Persistence of a groundwater contaminant plume after hydraulic source containment at a chlorinated-solvent contaminated site, Groundwater Monit. Remed. 34 (2014) 23–32.
[13] Z. Guo, M.L. Brusseau, The impact of well-field configuration and permeability heterogeneity on contaminant mass removal and plume persistence, J. Hazard. Mater. 333 (2017) 109–115.
[14] A.F.B. Tompson, S.F. Carle, N.D. Rosenberg, R.M. Maxwell, Analysis of groundwater migration from artificial recharge in a large urban aquifer: a simulation perspective, Water Resour. Res. 35 (1999) 2981–2998.
[15] H.L. Lien, R.T. Wilkin, High-level arsenite removal from groundwater by zero-valent iron, Chemosphere 59 (2005) 377–386.
[16] V. Bichet, E. Grisey, L. Aleya, Spatial characterization of leachate plume using electrical resistivity tomography in a landfill composed of old and new cells (Belfort, France), Eng. Geol. 211 (2016) 61–73.
[17] W.D. Robertson, D.R. Van Stempvoort, J.W. Roy, S.J. Brown, J. Spoelstra, S.L. Schiff, D.R. Rudolph, S. Danielescu, G. Graham, Use of an artifi-cial sweetener to identify sources of groundwaternitrate contamination, Groundwater 54 (2016) 579–587.
[18] Alternatives for Managing the Nation's Complex Contaminated Groundwater Sites, NRC (National Research Council), Washington, D.C, 2013.
[19] R. Thiruvenkatachari, S. Vigneswaran, R. Naidu, Permeable reactive barrier for groundwater remediation, J. Ind. Eng. Chem. 14 (2) (2008) 145-15.
[20] F. Obiri-Nyarko, S.J. Grajales-Mesa, G. Malina, An overview of permeable reactive barriers for in situ sustainable groundwater remediation, Chemosphere 111 (2014) 243–259.
[21] A. Erto, I. Bortone, A. Di Nardo, M. Di Natale, D. Musmarra, Permeable Adsorptive Barrier (PAB) for the remediation of groundwater simultaneously contaminated by some chlorinated organic compounds, J. Environ. Manage. 140 (2014) 111–119.
[22] G.F. Santonastaso, I. Bortone, S. Chianese, A. Di Nardo, M. Di Natale, A. Erto, D. Karatza, D. Musmarra, Discontinuous permeable adsorptive barrier design and cost analysis: a methodological approach to optimization, Environ. Sci. Pollut. Res. -

Int. 25 (27) (2018) 26793–26800.
[23] G.F. Santonastaso, A. Erto, I. Bortone, S. Chianese, A. Di Nardo, D. Musmarra, Experimental and simulation study of the restoration of a thallium (I)-contaminated aquifer by Permeable Adsorptive Barriers (PABs), Sci. Total Environ. 630 (2018) 62–71.
[24] A.D. Henderson, A.H. Demond, Long-term performance of zero-valent iron permeable reactive barriers: a critical review, Environ. Eng. Sci. 24 (2007) 401–423.
[25] R.C. Borden, Concurrent bioremediation of perchlorate and 1,1,1-trichloroethane in an emulsified oil barrier, J. Contam. Hydrol. 94 (1–2) (2007) 13–33.
[26] V. Zolla, F.S. Freyria, R. Sethi, A. Di Molfetta, Hydrogeochemical and biological processes affecting the long-term performance of an iron-based permeable reactive barrier, J. Environ. Qual. 38 (3) (2009) 897–908.
[27] G.E. Fogg, S.F. Carle, C. Green, Connected-network paradigm for the alluvial aquifer system, in: D. Zhang, C.L. Winter (Eds.), Theory, Modeling, and Field Investigation in Hydrogeology: A Special Volume in Honor of Shlomo P. Neuman'S 60th Birthday, Boulder, Colorado. Geologic. Soc. Am. (Special Paper), 348 2000, pp. 25–42.
[28] E.M. LaBolle, G.E. Fogg, Role of molecular diffusion in contaminant migration and recovery in an alluvial aquifer system, Transp. Porous Media 42 (2001) 155–179.
[29] S.F. Carle, A Transition Probability-based Approach to Geostatistical Characterization of Hydrostratigraphic Architecture, Ph. D. dissertation University of California, Davis, 1996, p. 248.
[30] S.F. Carle, G.E. Fogg, Transition probability-based indicator geostatistics, Math. Geol. 28 (1996) 453–477.
[31] S.F. Carle, G.E. Fogg, Modeling spatial variability with one- and multi-dimensional continuous Markov chains, Math. Geol. 29 (1997) 891–917.
[32] S.F. Carle, E.M. LaBolle, G.S. Weissmann, Van D. Brocklin, G.E. Fogg, Conditional simulation of hydrofacies architecture: a transition probability/Markov chain approach, in hydrogeologic models of sedimentary aquifers, concepts hydrogeol, in: G.S. Fraser, J.M. Davis (Eds.), Environ. Geol. Ser. vol. 1, Soc. of Sediment. Geol., Tulsa, Okla, 1998, pp. 147–170.
[33] Z. Guo, G.E. Fogg, M.L. Brusseau, E.M. LaBolle, Lopez J, Case Study of Modeling the Contaminants Transport in Groundwater for a Site With Large Heterogeneity at Tucson. (2018) Unpublished.
[34] U.S. Environmental Protection Agency (U.S. EPA), Superfund: Progress at National Priority List Sites, Arizona and Nevada 1995 Update, Rep. EPA/540/R-95/073, Environ. Prot. Agency, Washington, D. C, 1995.
[35] Hughes Missile Systems Company, United States Air Force Plant 44, Groundwater remediation 1995 annual report, Tucson, Ariz., March 14, 1996.
[36] URS, Final-Annual Optimized Exit Strategy, Performance Metric Report, July 2014 to June 2015, OT012 – South of Los Reales Road, Regional Groundwater Plume, Air Force Plant 44, Tucson, Arizona. 2016.
[37] M.L. Brusseau, D.E. Matthieu III, K.C. Carroll, J. Mainhagu, C. Morrison, A. McMillan, A. Russo, M. Plaschke, Characterizing long-term contaminant mass discharge and the relationship between reductions in discharge and reductions in mass for DNAPL source areas, J. Contam. Hydrol. 149 (2013) 1–12.
[38] Phase II Investigation of Subsurface Conditions in the Vicinity of Abandoned Waste Disposal Sites, Hughes Aircraft Company Manufacturing Facility, Hargis and Montgomery, Inc., Tucson, Arizona, Vol. I. Tucson. AZ, 1982.
[39] N.T. Nelson, M.L. Brusseau, Field study of the partitioning tracer method for detection of dense nonaqueous phase liquid in a trichloroethene-contaminated aquifer, Environ. Sci. Tech. 30 (1996) 2859–2863.
[40] M.L. Brusseau, K.C. Carroll, T. Allen, J. Baker, W. DiGuiseppi, J. Hatton, C. Morrison, A. Russo, J. Berkompas, The Impact of in-situ chemical oxidation on contaminant mass discharge: linking source-zone and plume-scale characterizations of remediation performance, Environ. Sci. Technol. 45 (2011) 5352–5358.
[41] Z. Zhang, M.L. Brusseau, Characterizing three-dimensional hydraulic conductivity distributions using qualitative and quantitative geologic borehole data: application to a field site, Ground Water 36 (1998) 671–678.
[42] M.G. McDonald, A.W. Harbaugh, A Modular Three-dimensional Finite-difference Ground-water Flow Model, U.S. Geological Survey Techniques of Water-Resources Investigations, 1988, p. 586 Chapter A1.
[43] A.W. Harbaugh, E.R. Banta, M.C. Hill, M.G. McDonald, MODFLOW-2000, the U.S. Geological Survey modular ground-water model-user guide to modularization concepts and the ground-water flow process, U.S. Geological Survey Open-File Report (2000) 00–92.
[44] C. Zheng, MT3D: A Modular Three-dimensional Transport Model for Simulation of Advection, Dispersion, and Chemical Reactions of Contaminants in Groundwater Systems. Report 74280. U.S. EPA Robert S. Kerr Environmental Research Laboratory, Ada, OK, USA, 1990.